https://doi.org/10.15407/knit2024.04.048

A. BENALI, Ph.D., Assistant Professor
ORCID:0000-0002-8989-755X
E-mail: benabdel0305@gmail.com, abdelali.benali@univ-usto.dz

Automatic Departement, University of Sciences and Technology of Oran Mohamed BOUDIAF
1505 El M'naouer Oran, Algeria

WATER BODIES EXTRACTION USING MATHEMATICAL MORPHOLOGY

The management of water resources is vital for maintaining the world's ecosystems. Conventional methods of extracting water bodies remain very limited due to the complexity of the implementation. This leads to a reduction in the extraction precision. Our main objective is to improve the detection of water bodies. We tested the accuracy of our method on the Sentinel-2 Dataset that contains images with different complexity levels and heterogeneous structures like shadows, roads, buildings, etc.

This article presents an original method that implements the idea of separating the three-component RGB image matrices and then processing only the green matrix because it contains all water bodies with high precision. Our method is based mainly on the mathematical morphology. Firstly, we propose a simple and fast binary algorithm to detect the maximum of water bodies existing in the images. This step was carried out using the Hit-or-Miss Transform. The second step exploits applying the Top-Hat Transform to refine the segmentation result. By comparing our method with several currently used methods, we notice that our method improves the quality of segmentation and gives excellent results, which exceed 95% for all the metrics used to calculate the classification quality in the purview of remote sensing. The error obtained with our method remains less than 1 %. We can affirm that our method is very suitable for detecting bodies of water compared to all current methods.

Keywords: *water bodies, remote sensing, mathematical morphology, RGB, classification.*

1. INTRODUCTION

Water is essential for the survival of the human race, as well as nature. It provides essential ecosystem goods and services, preserves the balance of the earth, and supports economic development and the environment. Earth observation through satellites is now the main means of monitoring land plans.

Arash M. R. et al. [1] proposed a novel robust augmented normalized water index (ANDWI) using a solid line, RGB, NIR, and SWIR1-2 with dynamic thresholding (Otsu) method to improve the performance of ANDWI. Billson J. et al. [2] propose a solution to extract water bodies with a new approach of pixel category transplantation (PCT) for data augmentation. Bingxin B. et al. [3] developed a water flow method based on negative Bayesian distribution. This method determines the relationship between unconnected waters and does not rely on topographic data. Duan Y. et al. [4] use GaoFen-1D satellite data from Wuhan, Hubei Province, China, to extract water bodies with a new lightweight CNN named Lightweight Multi-Scale Land SurfaceWater Extraction Network (LMSWENet).

George B. et al. [5] proposed an improvement of the predictions made by the DeeplabV3+ model with a technique based on two-dimensional variational mode decomposition (2D-VMD). Gujrati A. et al.

Цитування: Benali A. Water bodies extraction using mathematical morphology. *Space Science and Technology.* 2024. **30**, No. 4 (149). P. 48—57. https://doi.org/10.15407/knit2024.04.048

[6] used the k-means cosine distance algorithm to detect and classify bodies of water according to their colors. Guru Prasad M. S. [7] trained the dataset downloaded from Kaggle with a deep CNN MSAA-Net hosted on TensorFlow. Hongye C. et al. [8] examined long-term changes in the open waters of the river basin from 2000 to 2020 using the Google Earth Engine (GEE) cloud platform to process 26,681 high-quality Landsat images. Jagruth K. [9] used mathematical morphology applied to pixel detection to detect water bodies. The problem of a method of this type is the slowness of the process. Jikang W. and Bin Y. [10] attempted to perform rapid and automatic water extraction over large areas using thermal infrared bands as input with a light detection neural network (EDCM) combined with an image classification model with a semantic segmentation model. They finally used the training of various models using lightweight convolutional networks to extract more data. Junjie L. et al. [11] used the technique of transitioning from label-free learning to noise-free learning.

Kalaivani K. et al. [12] used spatial frequency-based unattenuated wavelet transform (UDWT → SF) fusion to remove spectral information from images effectively. Then, they developed an efficient sub-pixel classification system using several prediction methods based on spectral characteristics. Kale S. et al. [13] reviewed the state of the art on water body extraction methods to predict the location of water resources. Lifu C. et al. [14] proposed a DNN framework for water body detection which consists of three parts: a water body extraction network with four pillars, a hybrid local and global association module (LGMA) for bone analysis, and activation of specific semantic categories, and a mapping module (SSAM) used for the high-level publishing process. Linrong L. et al. [15] used CDWI to improve water body extraction and removed shadows using SDWI. Liumeng C. et al. [16] work on monitoring the spatio-temporal characteristics of water bodies and studying the dynamic and regional effects of surface water changes. Liu Q. et al. [17] proposed detecting bodies of water using a method based on sparse superpixels (SSWE). Luo Y. et al. [18] used a generative adversarial network (GAN) to improve the characteristics of tiny water bodies, and they introduced band pooling into the DeepLabv3+ network for better extraction of water bodies.

Nguyen T. and Filipe A. [19] created a new global flood index with a resolution of 3 arcseconds based on ground data from the MERIT repository using neural networks. Parajuli J. et al. [20] developed a novel attentional dense convolutional neural network (AD-CNN) to help discover deeper features and dynamically emphasize the most relevant spatio-spectral features for water pixel classification. Sharma D. et al. [21] use principal component analysis (PCA) with thresholding to segment binary classes. Then, they apply erosion to improve the detection of water bodies. Suhail A.T. et al. [22] developed a simple and effective method for detecting bodies of water based on the Marr-Hildreth method merged with Canny Edge. Sunandini G. et al. [23] developed a comparative study on the performance of the Deeplabv3+ model with ASPP and without ASPP for the segmentation of water bodies. Wenxue X. et al. [24] used the Google Earth Engine (GEE) platform to create an annual water map in Shandong Province from 1990 to 2020 to analyze the distribution and change of surface water. Xue W. et al. [25] propose extracting water bodies using a model called a dense coordinate feature concatenation network. Xu N. et al. [26] used all data available on Google Earth Engine to detect water bodies across Australia.

Benkesmiaa Y. et al. [27] studied the water level changes (SWE) in Grand Sebkha, Oran (GSO), a wetland located on the border of the city of Oran. Youzhi L. et al. [28] developed a method based on multilevel filtering to minimize noise pixels and then extract water surface pixels using a modified alpha form to derive water level elevation. Yuanhui Z. et al. [29] used data from Research on Science and Climate Change (GRACE) and the Global Land Data System (GLDAS) to analyze changes in groundwater and surface water (GSW) bodies in Canadian provinces between 2002 and 2016. Zhang Z. et al. [30] consider pixel intensity and spatial correlation between neighboring pixels using deep learning-based models for water body extraction. Other researchers like Rishikeshan C. A. and Ramesh H. [31] have used mathematical morphology for Shoreline detection. The use of mathematical morphology in image processing allows one to reduce processing time.

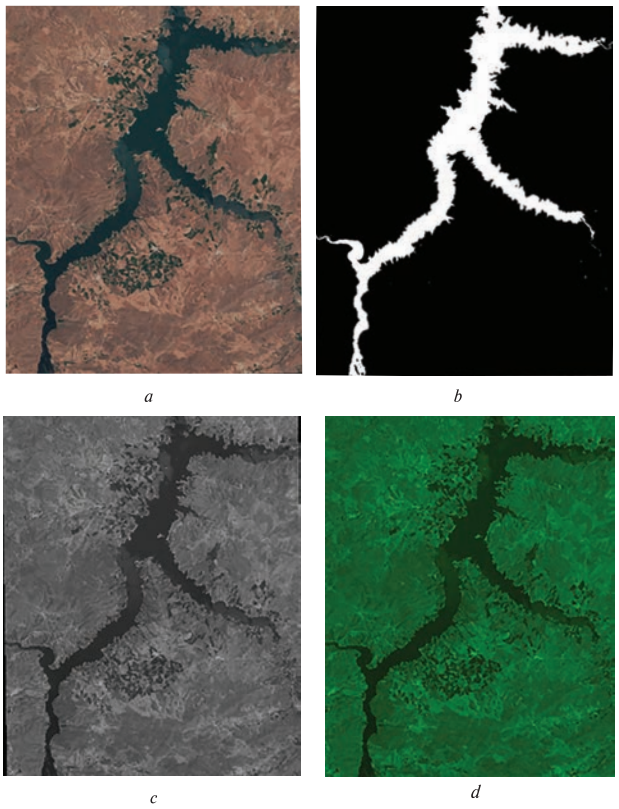

Figure 1. Images used as input: *a* — original satellite image, *b* — the mask image, *c* — the gray scale image for the green matrice, *d* — the green matrice image

The originality of our work lies in the separation of three RGB spectral components of the satellite image and the subsequent application of individual processing for the Green matrix only. We decided to use mathematical morphology because it is simple to implement, effective in providing a good detection rate, and, above all, allows us to reduce processing time.

2. DATA USED

To evaluate the effectiveness of our method, we prepared 100 complex images from the Sentinel-2 database that we downloaded from Kaggle, the data was collected via the Sentinel-2 API. The images have been pre-processed using Rasterio software. The images show different types of water bodies in different regions. Each of these images is accompanied by a black-and-white mask where white color represents water, and black represents non-aquatic regions. The generation of masks was carried out by calculating the NDWI (Normalized Difference Water Index) derived from bands 8 and 3 of the satellite, which is frequently used to detect and measure vegetation in satellite images, but for bodies of water, we used a higher threshold.

Figure 1 shows the input images used in our method to extract water bodies.

The three RGB matrices of the original image are separated. We keep only the Green matrix because it is better suited for detecting water bodies. We then apply our method to the grayscale image of the Green matrix.

3. METHODS

This article presents a new unsupervised method based on mathematical morphology operators for automatically extracting water bodies from satellite images. The different steps of our method are illustrated in the flowchart presented in Figure 2.

3.1. To remove the majority of pixels from non-aquatic regions, we apply a Top-Hat Transform (TH) as follows:

a. Morphological closure applied to the original image.

b. Subtract between the initial image and the result of the first step.

$$I_f = I \bullet E = \left(I \oplus E\right) \ominus E, \tag{1}$$

$$I_{chf} = I - I_f, \tag{2}$$

with: I_f — result of the morphological closing applied to the initial image (I), $\oplus$ — the dilation operator, $\ominus$ — erosion operator, I — the initial image, E — the structuring element.

3.2. To eliminate non-important structures such as buildings, roads, or trees, we applied hysteresis thresholding.

$$I_{low} = \begin{cases} 1 \text{ pour } I \geq \text{Slow}, \\ 0 \text{ pour } I < \text{Slow}, \end{cases} \tag{3}$$

$$I_{high} = \begin{cases} 1 \text{ pour } I \leq \text{Shigh}, \\ 0 \text{ pour } I > \text{Shigh}, \end{cases} \tag{4}$$

$$It = Ilow^{*}Ihigh, \tag{5}$$

with: I_{low} — the resulting image after applying the low threshold, I_{high} — the resulting image after applying the high threshold, It — the resulting image after the application of hysteresis thresholding.

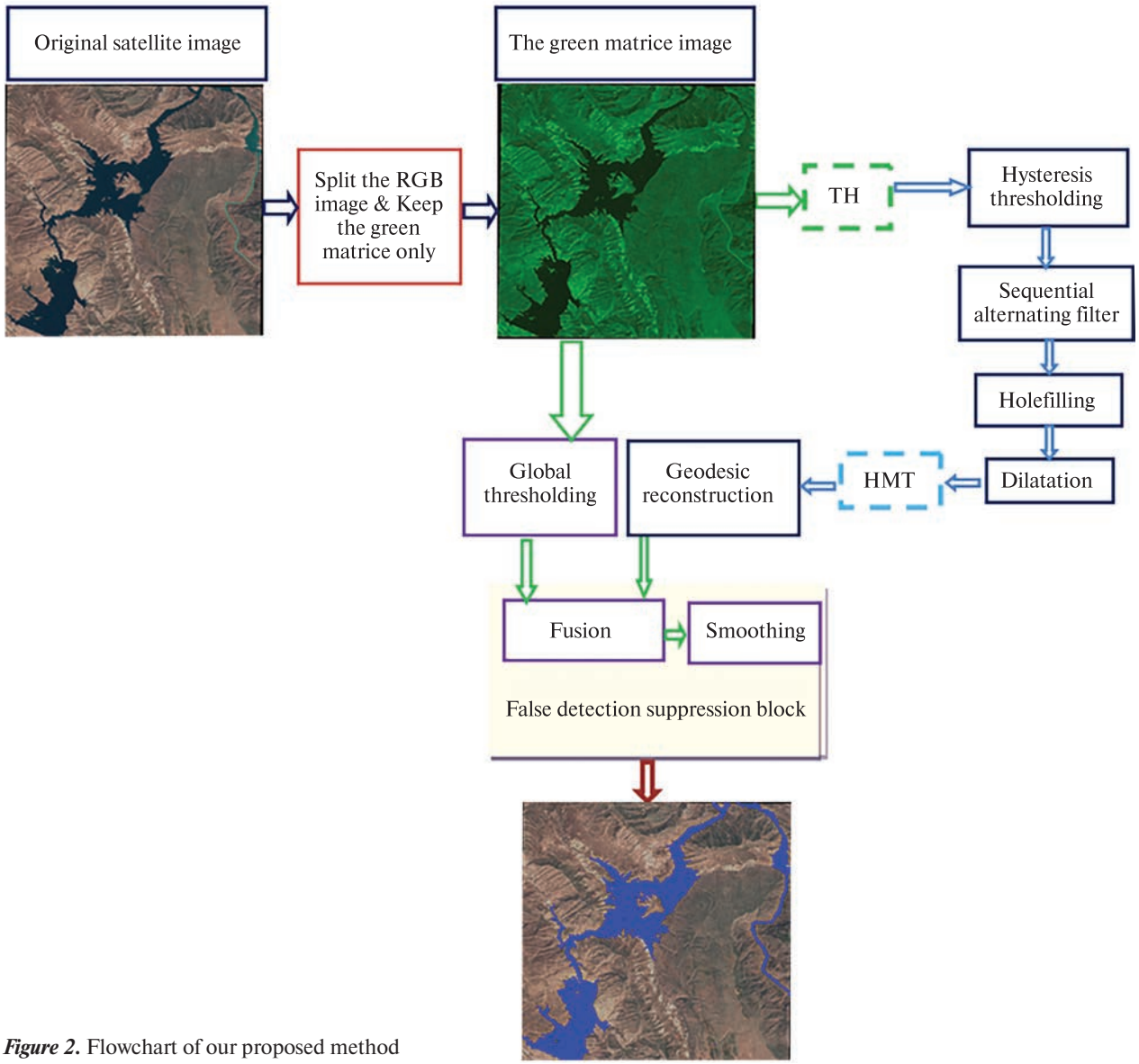

Figure 2. Flowchart of our proposed method

3.3. For noise elimination, we used a sequential alternating filter. Alternating filters are obtained with combinations of closings (•) and openings (◦):

$$\varphi_k(\mathrm{It}) = (\mathrm{It} \bullet \mathrm{B}_k) \circ \mathrm{B}_k, \quad (6)$$

$$\mathrm{I}_{f\,K}(\mathrm{It}) = \varphi_k \varphi_{k-1} \ldots \varphi_1(\mathrm{It}), \quad (7)$$

with: B — structuring element of the filter, K — the filter size, I_f — the resulting image is obtained by sequential alternating filtering.

3.4. The hole-filling process is achieved in four stages. They are the next :

• Complementation of the initial binary image.

• Labeling connected components to distinguish between the objects of interest.

• Assigning the value of 0 to the pixels of these regions.

• Complementation of the result to recover segments of our class of water bodies.

3.5. The last step of preprocessing is the application of dilation to correct deformations generated by the different morphological operators, which can distort the shape of the regions belonging to the water

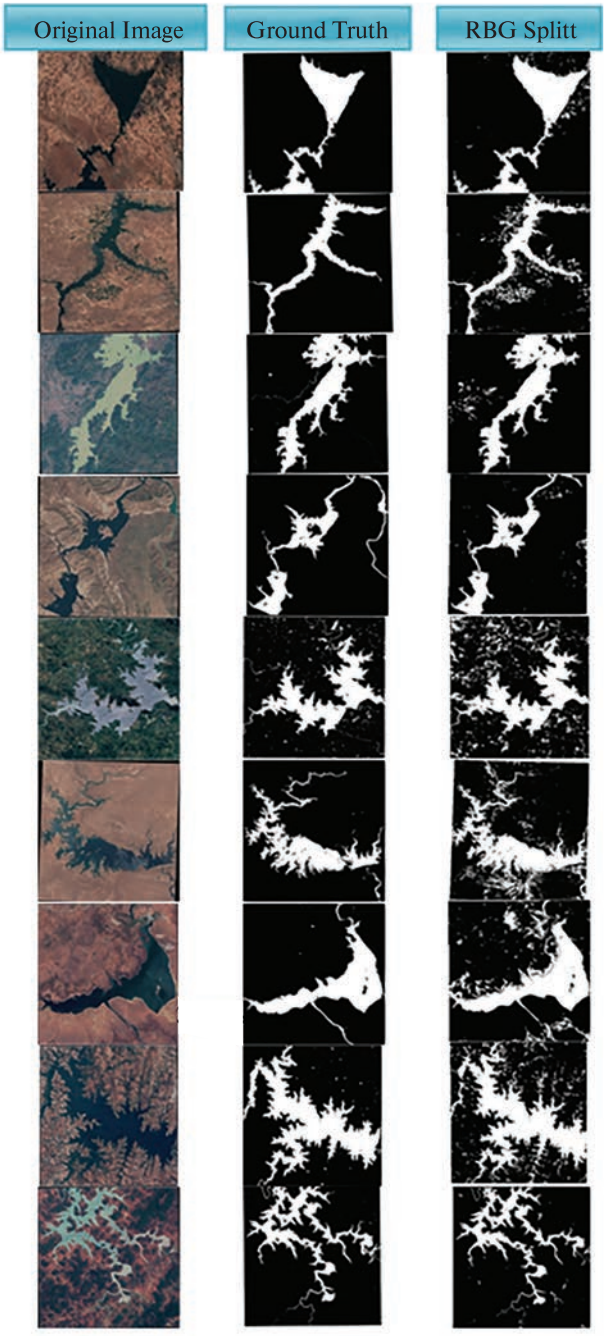

Figure 3. Results of water body extraction for images from the Sentinel-2 dataset

bodies' class and possibly cause the loss of some areas of water bodies of our class.

$$I_d = I \oplus E, \tag{8}$$

with: I_d — the result obtained after applying dilation. $\oplus$ — the dilation designator.

3.6. The extraction of water bodies is carried out using the Hit-or-Miss Transform (HMT):

$$A \otimes (E,F) = (A \ominus E) \cap (A^c \ominus F), \tag{9}$$

with: $\otimes$ — the Hit-or-Miss Transform designator, $\ominus$ — the erosion designator, E, F — the structuring elements.

The transform consists of extracting all the regions of the water-bodies class whose size varies between the size of the structuring element E and that of F.

3.7. Restoration of the shapes of water bodies by geodesic reconstruction. The distortion of water body shapes is significant after applying HMT, which requires us to apply a reconstruction step to restore the original shapes of water bodies.

The reconstruction requires a marker image that corresponds to the result obtained by the HMT. A succession of dilations is applied to the marker image. Finally, the result obtained will be conditioned by the Ie mask.

$$I_{rec} = \left(I_{hmt} \oplus_{I_{smo}} C_i \right)^{\infty} \tag{10}$$

With an application of conditional dilation until the result of the transformation is invariant:

$$I_{hmt} \oplus_{I_{smo}} C_i = (I_{hmt} \oplus C_i) \cap I_{smo}, \tag{11}$$

with: I_{rec} — result of geodesic reconstruction, I_{hmt} — the HMT resulting image, C_i — the structuring elements of the geodesic reconstruction ($1 \le i \le 3$), I_{smo} — result after smoothing.

3.8. Block to remove extraction errors and false detections. Since we are using an unsupervised approach, we will have to construct a reference image by applying global thresholding. The result of our extraction method will be conditioned by the reference image to reduce false detections.

After the conditioning step, we will apply morphological smoothing to remove the remaining false detections.

$$I_{fus} = I_{rec} \cap I_{seg}, \tag{12}$$

with: I_{fus} — the resulting image from the fusion, I_{seg} — result of global thresholding.

3.9.The morphological smoothing

$$I_{smo} = I_{fus} \circ N = \left(I_{fus} \ominus N\right) \oplus N, \qquad (13)$$

with: I_{smo} — result of applying smoothing on the conditioned image, N — structuring element.

The size of the structuring elements used in our method for all operations is chosen experimentally and varies for each of the images depending on the size of the water bodies existing in each image and depending on the background and especially the size of the trees, buildings, or road that need to be removed.

4. EXPERIMENTS AND RESULTS

We tested our method on the entire RGB image. Then, we tested our method on each of the RGB matrices separately. We found that the best extraction results for bodies of water were obtained with the Green matrix, given that the color of the regions belonging to the water-bodies class is very close to those existing in the green matrix.

We applied our method to the Sentinel-2 Dataset. Figure 3 illustrates the extraction results.

4.1. ***Accuracy assessment***. Below, we give a comparative table showing the water body extraction results of our method compared to many other currently applied methods with the most popular evaluation criteria used in remote sensing.

$$\text{Precision} = \frac{TP}{TP + FP}$$

$$\text{Recall} = \frac{TP}{TP + FN}$$

$$\text{F1} = 2 * \frac{Precision * Recall}{Precision + Recall}$$

$$\text{OA} = \text{OA} = \frac{TP + TN}{TP + FP + TN + FN}$$

$$\text{IOU} = \frac{TP}{TP + FP + FN}$$

$$\text{PA} = \frac{TN}{TN + FP}$$

$$\text{UA} = \text{UA} = \frac{TN}{TN + FN}$$

$$\text{Kappa} = \frac{OA - Pe}{1 - PE}$$

Table 1. **Evaluation of extraction results with the most used criteria for remote sensing**

	Jag21	Junj22	Jik23	Lin21	Lif23	Gur23	Jana22	Zhi21	Yua22	Bic23	Yue21	Jos23	Gos23	Qin22	Wei21	Our Method
Precision	69.38	98.16				98.24					86.45	73.02	90			98.8
Recall	74.54	95.41				98.12	83		93.87		94.12	68.02	95			99.8
F1		96.76				98.66		90.21		47	90.14		92		94.7	99.3
PA			93.90	83.55	95.70				94.72		95.93			94.68		98.8
UA			96.01	99.97										95.05		99.8
OA	76.97		95.20	91.78		98.93	89.66	98.4						98.91	98.95	99.3
Kappa				84.61										94.2		98.6
Iou					91.91			83.31			82.05				90.12	98.6
Mean-Iou						97.26			93.16		88.53	75.42				98.6
Jaccard										34			86			98.6
ER											4.07					0.7
MPI											92.50					99.3

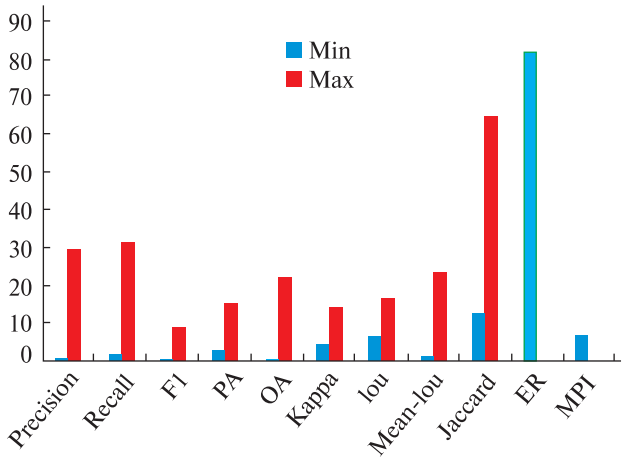

Figure 4. Improvement in results obtained with the different evaluation criteria for our method compared to other methods

Where:

$$Pe = \frac{(TP+FP)*(TP+FN)+(TN+FP)*(TN+FN)}{(TP+TN+FP+FN)^2}$$

$$\text{Jaccard} = \frac{TP}{TP+FN+FP}$$

$$\text{ER} = \frac{FP+FN}{TP+TN+FP+FN}$$

$$\text{MP} = \frac{1}{n+1}\sum_{i=0}^{n}\frac{TP}{TP+FP}$$

$$\text{MIOU} = \frac{1}{n+1}\sum_{i=0}^{n}\frac{TP}{TP+FP+FN}$$

where: *TP* — true Positive, *TN* — true Negative, *FP* — false Positive, *FN* — false Negative.

From Table 1, we can affirm that our method is better than other water body detection methods. Traditional algorithms and detection algorithms still cannot solve the problem of interference between regions belonging to the class of water bodies and buildings or roads.

During the process of extracting bodies of water, other algorithms appear to have misidentified many houses, roads, farms, and mountains as bodies of water. Indeed, bodies of water are sometimes found in high mountains.

As shown in Table 1, all evaluation criteria indicate that our method outperforms other methods in extracting water bodies.

The experimental results confirm that our method improved the extraction quality of water bodies.

5. DISCUSSION

From Figure 3, we observe that our method allowed us to extract almost all regions of the water-bodies class with low detection errors for almost all complex images.

In this work, we focused on two points. The first is to have high accuracy in detecting water bodies, and the second is to minimize the processing time.

The use of Mathematical Morphology allowed us to minimize the processing time compared to all current methods, especially those that use deep learning. Our method takes less processing time for large images because Mathematical Morphology is well suited for quickly processing large dimensional matrices.

Good detection was also guaranteed with the use of Mathematical Morphology applied to the green matrix because all the satellite images present water bodies that have a color close to the pixel intensity of the regions belonging to the planes class of waters existing in the green matrix, which allowed us to detect most bodies of water with a minimum of false detections.

The processing time for each image does not exceed 2 minutes, which is excellent for processing datasets containing a large number of images of large dimensions.

We calculated the rate of improvement of the factors for each of the evaluation criteria and constructed a comparative diagram to show the effectiveness of our method. From Figure 4, we observe that our method provides 0.5—29 % improvement in precision, 1.6—31 % improvement in recall, 0.6—9.2 % improvement in F1-score, 2.9—15.4 % improvement in PA, 0.35—22.4 % improvement in OA, 4.4—14.1 % improvement in Kappa, 6.7—16.7 % improvement in IoU, 1.3—23.5 % improvement in Mean-IoU, 12.7—65.5 % improvement in Jaccard, 82.8 % improvement in ER, and 6.8 % improvement in MPI.

With all the improvements in water-body detection, we confim that our method yields better results than other existing methods.

6. CONCLUSIONS

The originality in this article is the use of the green matrix after the separation of the three RGB components of the image. We have carried out an unsupervised automatic extraction of water bodies from RGB satellite images and have applied our method to the Sentienl-2 Database.

We compared the accuracy of the results of our method with many current methods, especially those using deep learning. We found that our method requires less processing time and gives the best qualitative rate using most evaluation criteria used in the purview of remote sensing.

Our contribution allowed the detection of all regions belonging to the water bodies class existing in the images of our database, even water bodies existing in images with a complex background, without detecting roads, buildings, trees, etc.

The rate exceeded 95 % for almost all the evaluation criteria used, and the detection error is less than 1 %, which is excellent for the future of remote sensing, in particular for the extraction of water plan data.

From this perspective, we will use our method for road detection, and aim to combine it with deep learning and other thresholding techniques to achieve better results.

Declaration of Competing Interest: *Benali Abdelali declares that he has no known competing financial interests or personal relationships that could have appeared to influence the work reported in this paper.*

Data availability: *Data will be made available on request.*

Acknowledgments: *The author would like to thank the anonymous reviewers for their valuable comments that substantially improve the quality of this paper.*

REFERENCES

1. Arash Modaresi Rad, Jason Kreitler, Mojtaba Sadegh (2021). Augmented Normalized Difference Water Index for Improved Surface Water Monitoring. *Environmental Modelling & Software,* **140**, 105030—105076.
2. Billson Joshua, MD Samiul Islam, Xinyao Sun, and Irene Cheng (2023). Water Body Extraction from Sentinel-2 Imagery with Deep Convolutional Networks and Pixelwise Category Transplantation. *Remote Sensing*, **15**, No. 5, 1253—1270. https://doi.org/10.3390/rs15051253
3. Bingxin Bai, Yumin Tan, Gennadii Donchyts, Arjen Haag, Bo Xu, Ge Chen, Albrecht H. Weerts (2023). Naive Bayes classification-based surface water gap-filling from partially contaminated optical remote sensing image. *J. Hydrology*, **616**, 128791—123803.
4. Duan Yueming, Wenyi Zhang, Peng Huang, Guojin He, and Hongxiang Guo (2021). A New Lightweight Convolutional Neural Network for Multi-Scale Land Surface Water Extraction from GaoFen-1D Satellite Images. *Remote Sensing*, **13**, No. 22, 4576—4598. https://doi.org/10.3390/rs13224576
5. George Bichu, Sajith Variyar V. V, Sowmya V. and Sivanpillai Ramesh (2023). Performance Improvement of Water Body Segmentation by DeeplabV3+Using Two Dimensional Variational Mode Decomposition. *10th Int. Conf. on Signal Processing and Integrated Networks (SPIN)*, Noida, India, 603—608. doi: 10.1109/SPIN57001.2023.10116311
6. Gujrati Ashwin, Jha Vibhuti Bhushan, Nidamanuri, Rama Rao, Singh. R. P. (2023). Satellite-based Optical Water Type Classification of Inland Waters Bodies of India. I*nt. Conf. Machine Intelligence for GeoAnalytics and Remote Sensing (MIGARS),* Hyderabad, India, 1—4. doi: 10.1109/MIGARS57353.2023.10064493
7. Guru Prasad M. Agarwal Jyoti, Christa Sharon, Aditya Pai H., Kumar M. A. and Kukreti Anand, Anurag Kukreti (2023). An Improved Water Body Segmentation from Satellite Images using MSAA-Net. *Int. Conf. Machine Intelligence for GeoAnalytics and Remote Sensing (MIGARS)*, Hyderabad, India, 1—4. doi: 10.1109/MIGARS57353.2023.10064508
8. Hongye Cao, Ling Han, Liangzhi Li (2022). Changes in extent of open-surface water bodies in China's Yellow River Basin (2000—2020) using Google Earth Engine cloud platform. *Anthropocene,* **39**, 100346—100359.
9. Jagruth K., V. Manikandan M., and Kumar Ravi Kant (2021). Water Body Identification from the Satellite Images using Color Component Analysis with Morphological Operations. *12th ICCCNT* (2021 - IIT - Kharagpur Kharagpur, India).
10. Jikang Wan and Bin Yong (2023). Automatic extraction of surface water based on lightweight convolutional neural network. *Ecotoxicology and Environmental Safety*, **256**, 114843—114854.
11. Junjie Li, Yizhuo Meng, Yuanxi Li, Qian Cui, Xining Yang, Chongxin Tao, Zhe Wang, Linyi Li and Wen Zhang (2022). Accurate water extraction using remote sensing imagery based on normalized difference water index and unsupervised deep learning. *J. Hydrology*, **612**, 128202—128216.

12. Kalaivani Kathirvelu, Asnath Victy Phamila Yesudhas, Sakkaravarthi Ramanathan (2023). Spectral unmixing based random forest classifier for detecting surface water changes in multitemporal pansharpened Landsat image. *Expert Systems With Applications*, **224**, 120072—120086.
13. Kale Suhas, Gawali Bharti, Shafiyoddin Sayyad (2021). Extraction of Water Bodies in Godawari Basin from Satellite Images. *IEEE Int. India Geoscience and Remote Sensing Symp. (InGARSS),* Ahmedabad, India, 141—144. doi: 10.1109/InGARSS51564.2021.9792088
14. Lifu Chen, Xingmin Cai, Jin Xing, Zhenhong Li, Wu Zhu, Zhihui Yuan, Zhenhuan Fang (2023). Towards transparent deep learning for surface water detection from SAR imagery. *Int. J. Appl. Earth Observation and Geoinform.*, **118**, 103287—103302.
15. Linrong Li, Hongjun Su, Qian Du, Taixia Wu (2020). A novel surface water index using local background information for long term and large-scale Landsat images. *ISPRS J. Photogrammetry and Remote Sensing*, **172**, 59—78.
16. Liumeng Chen, Yongchao Liu, Jialin Li, Peng Tian, Haitao Zhang (2023). Surface water changes in China's Yangtze River Delta over the past forty years. *Sustainable Cities and Society*, **91**, 104458—104474.
17. Liu Qingwei, Tian Yugang, Zhang Lihao, and Chen Bo (2022). Urban Surface Water Mapping from VHR Images Based on Superpixel Segmentation and Target Detection. *IEEE J. Selected Topics in Appl. Earth Observ. and Remote Sensing*, **15**, 5339—5356. doi: 10.1109/JSTARS.2022.3181720
18. Luo Yuanjiang, Feng Ao, Li Hongxiang, Li Danyang, Xuan Wu, Liao Jie, Zhang Chengwu, Zheng Xingqiang, Pu Haibo (2022). New deep learning method for efficient extraction of small water from remote sensing images. *PLoS ONE*, **17**(8), e0272317. https://doi.org/10.1371/journal.pone.0272317
19. Nguyen Thu-Hang, Filipe Aires (2023). A global topography- and hydrography-based floodability index for the downscaling, analysis, and data-fusion of surface water. *J. Hydrology*, **620**, 129406—129421.
20. Parajuli Janak, Ruben Fernandez-Beltran, Jian Kang and Filiberto Pla (2022). Attentional Dense Convolutional Neural Network for Water Body Extraction From Sentinel-2 Images. *IEEE J. Selected Topics in Appl. Earth Observ. and Remote Sensing*, **15**, 6804—6816. doi: 10.1109/JSTARS.2022.3198497
21. Sharma Deepa, Trapti Sharma and Jyoti Singhai (2021). Extraction of Water Bodies from Visible Color Satellite Images Using PCA Feature Map. *IEEE Int. India Geosci. and Remote Sensing Symp. (InGARSS)*, Ahmedabad, India, 1—4. doi: 10.1109/InGARSS51564.2021.9791857
22. Suhail Ahamed T., Nalini N. and Rimlon Shibi S. (2023). Edge Detection of Satellite Image for Water Body Identification using Marr -Hildreth Algorithm and comparing with Canny edge Detector Algorithm to Enhance Accuracy and Contrast. *Eighth Int. Conf. on Sci. Technology Engineering and Mathematics* (ICONSTEM), Chennai, India, 1—5. doi: 10.1109/ICONSTEM56934.2023.10142577
23. Sunandini Gosula, Sivanpillani Ramesh, Sowmya V. and Variyar Sajith V. V. (2023). Significance of Atrous Spatial Pyramid Pooling (ASPP) in Deeplabv3+ for Water Body Segmentation. *10th Int. Conf. on Signal Processing and Integrated Networks* (SPIN), Noida, India, 744—749. doi: 10.1109/SPIN57001.2023.10116882
24. Wenxue Xing, Bin Guo, Yingwu Sheng, Xingchao Yang, Min Ji, Ying Xu (2022). Tracing surface water change from 1990 to 2020 in China's Shandong Province using Landsat series images. *Ecological Indicators*, **140**, 108993—109001. https://doi.org/10.1016/j.ecolind.2022.108993
25. Xue Weibao, Hui Yang, Yanlan Wu, Peng Kong, Hao Xu, Penghai Wu, and Xiaoshuang Ma. (2021). Water Body Automated Extraction in Polarization SAR Images With Dense-Coordinate-Feature-Concatenate Network. *IEEE J. Selected Topics in Appl. Earth Observ. and Remote Sensing*, **14**, 12073—12087. doi: 10.1109/JSTARS.2021.3129182
26. Xu Nan, Yue Ma, Wenhao Zhang, and Xiao Hua Wang (2021). Surface-Water-Level Changes During 2003—2019 in Australia Revealed by ICESat/ICESat-2 Altimetry and Landsat Imagery. *IEEE Geosci. and Remote Sensing Lett.*, **18**, No. 7, 1129—1133. doi: 10.1109/LGRS.2020.2996769
27. Yamina Benkesmia, Moulay Idriss Hassani, and Cherif Kessar (2023). Variation of surface water extent in the great Sebkha of Oran (NW of Algeria), using Landsat data 1987—2019: Interaction of natural factors and anthropogenic impacts. *Remote Sensing Appl.: Society and Environment*, **30**, 100953—100972.
28. Youzhi Li, Zhihua Mao, Zhenge Qiu, Kuifeng Luan, Bangyi Tao, Haiqing Huang, and Chunling Zhang (2023). Algorithm for Detection of Water Surface Height in UAV-Borne Photon-Counting LiDAR. *IEEE Geosci. and Remote Sensing Lett.*, **20**, 6500605—6500609.
29. Yuanhui Zhu, Soe W. Myint, Danica Schaffer-Smith, David J. Sauchyn, Xiaoyong Xu, Joseph M. Piwowar, and Yubin Li (2022). Examining ground and surface water changes in response to environmental variables, land use dynamics, and socio-economic changes in Canada. *J. Environmental Management*, **322**, 115875—115884.
30. Zhang Zhixin, Da Liu, Zhe Liu, Yanjun Qiao, Changan Zheng, and Yong Gan (2021). Deep learning based methods for water body extraction and flooding evolution analysis based on Sentinel-1 images. *7th Int. Conf. on Hydraulic and Civil Engineering & Smart Water Conservancy and Intelligent Disaster Reduction Forum* (ICHCE & SWIDR), Nanjing, China, 191—195. doi: 10.1109/ICHCESWIDR54323.2021.9656266

31. Rishikeshan C. A., Ramesh H. (2017). A novel mathematical morphology based algorithm for shoreline extraction from satellite images. *Geo-Spatial Inform. Sci.*, **20**(4), 345—352. https://doi.org/10.1080/10095020.2017.1403089

Стаття надійшла до редакції 15.03.2024 *Received 15.03.2024*
Після доопрацювання 03.06.2024 *Revised 03.06.2024*
Прийнято до друку 09.06.2024 *Accepted 09.06.2024*

А. Беналі, д-р філософії, доцент
ORCID: 0000-0002-8989-755X
E-mail: benabdel0305@gmail.com, abdelali.benali@univ-usto.dz

Відділення автоматики Оранського університету наук і технології Мохаммеда Будіафа
1505 Ель Мнауер, Оран, Алжир

ВИЛУЧЕННЯ ВОДНИХ ОБ'ЄКТІВ ЗА ДОПОМОГОЮ МАТЕМАТИЧНОЇ МОРФОЛОГІЇ

Управління водними ресурсами є життєво важливим для збереження світових екосистем. Традиційні методи ототожнення водних об'єктів на зображеннях залишаються дуже обмеженими через складність реалізації. Це призводить до зниження точності ідентифікації. Наша основна мета — покращити виявлення водних об'єктів. Ми протестували точність нашого методу на наборі даних Sentinel-2, який містить зображення з різними рівнями складності та неоднорідними структурами, такими як тіні, дороги, будівлі тощо.

У статті представлено оригінальний метод, який реалізує ідею розділення трикомпонентних матриць RGB-зображень і подальшої обробки лише «зеленої» матриці, оскільки вона містить усі водні об'єкти з високою точністю. Наш метод базується в основному на математичній морфології. По-перше, ми пропонуємо простий і швидкий бінарний алгоритм для виявлення максимальної кількості водойм, що наявні на зображеннях. Цей крок було виконано за допомогою перетворення «влучив-не-влучив» (Hit-or-Miss Transform). На другому кроці для уточнення результату сегментації використовується перетворення Top-Hat для визначення максимальної кількості водойм. Порівнюючи наш метод з кількома методами, що використовуються в даний час, ми помітили, що наш метод покращує якість сегментації і дає відмінні результати, які перевищують 95 % для всіх метрик, що використовуються для розрахунку якості класифікації в галузі дистанційного зондування. Похибка, отримана за допомогою нашого методу, становить менш ніж 1 %. Можна стверджувати, що наш метод дуже добре підходить для виявлення водойм серед інших відомих методів.

Ключові слова: водойми, дистанційне зондування, математична морфологія, RGB, класифікація.